Acta Cryst. (1995). D**51**, 168–176

Structure of the Azurin Mutant Phe114Ala from *Pseudomonas aeruginosa* at 2.6 Å Resolution

BY LI-CHU TSAI,* LENNART SJÖLIN AND VRATISLAV LANGER

Department of Inorganic Chemistry, Chalmers University of Technology and The University of Göteborg, S-142 96 Göteborg, Sweden

TORBJÖRN PASCHER

Department of Biochemistry and Biophysics, The University of Göteborg, S-142 96 Göteborg, Sweden

AND HERBERT NAR

Max Planck Institut für Biochemie, Abteilung für Struktur Forschung, Martinsried bei München, Germany

(*Received* 3 *February* 1994; *accepted* 20 *May* 1994)

Abstract

The crystal structure of azurin mutant Phe114Ala from *Pseudomonas aeruginosa* has been solved by molecular replacement. The final crystallographic R value is 0.185 for 9832 reflections to a resolution of 2.6 Å. The root-mean-square deviation for main-chain atom positions is 0.020 Å between the four independent monomers in the asymmetric unit. The mutant Ala114 crystallized from PEG 4000 in a new crystal form and the crystals are monoclinic, $P2_1$, $a = 51.0$, $b = 83.6$, $c = 66.4$ Å and $\beta = 110.5°$. The four molecules in the asymmetric unit are packed as a dimer of dimers and are related by an approximate twofold axis. The dimer packing and the dimer contact region are very similar to that of the *Alcaligenes denitrificans* azurin dimer. The mutation was performed at residue Phe114, which exhibits a π-electron overlap with the copper ligand His117, to investigate its suggested role in the electron self-exchange reaction. Removal of steric constrains from the phenylalanine side chain created a somewhat different geometry around the copper site with an increased mobility of His117 resulting in an enlarged Cu—N length which may be responsible for the slight differences obtained in the spectral properties of the mutant *versus* the wild-type protein.

Introduction

Azurin from *Pseudomonas aeruginosa* is a small (M_r 14000) electron-mediating type I blue-copper protein. It has been known for a long time that azurin plays a central role in bateria where it receives an electron from cytochrome c_{551} and delivers the electron to nitrite reductase. In addition, azurin has distinctive spectroscopic properties and high redox potential ($\lambda \simeq 600$ nm, $\varepsilon \simeq 5600\ M^{-1}\ cm^{-1}$, $E^{\ominus} \simeq$ 300–400 mV).

Although the sequence homology is rather low between different classes of cupredoxins, there is a high degree of structural similarity. All the copper-containing proteins characterized by X-ray diffraction thus far contain at least one Greek-key β-barrel domain, maybe representing a distant evolutionary relationship among them (Adman, 1991). This motif is also present in the three subunits of ascorbate oxidase and in human factor V and VIII from the blood-clotting system (Messerschmidt & Huber, 1990; Rydén, 1988). The type I copper-site geometry is highly conserved in these proteins. From crystallographic studies on plastocyanin (Guss & Freeman, 1983), *Alcaligenes denitrificans* azurin (Norris, Anderson & Baker, 1986) and *P. aeruginosa* azurin (Adman & Jensen, 1981; Nar, Messerschmidt, Huber, van de Kamp & Canters, 1991*a*; Karlsson, Tsai, Nar, Langer & Sjölin, 1994) a canonical copper-site geometry has been concluded.

The *P. aeruginosa* azurin molecule consists of a single polypeptide chain of 128 amino-acid residues plus one Cu atom. The Cu site lies about 7 Å below the surface and is coordinated by five ligands, three equatorial ligands, His46, Cys112 and His117, and two weak ligands in axial positions, Gly45 and Met121. This geometry, the carbonyl O atom excepted, is conserved in all known structures of type I copper determined so far. The interaction between copper and the axial methionine ligand has been suggested as an important factor for the fine tuning of the reduction potential (Gray & Malmström, 1983; Norinder, Sjölin, Pascher & Karlsson, 1994).

A number of attempts have previously been carried out in order to investigate the specific role of

* Author for correspondence.

©1995 International Union of Crystallography
Printed in Great Britain – all rights reserved

the copper ion and also its role in the electron-transfer mechanism between different metalloproteins. In these investigations inorganic redox agents like chromium, ruthenium and iron compounds have been used in order to study different aspects of the phenomenon (Antonini, Finazzi-Agro, Avigliano, Guerrieri, Rotilio & Mondovi, 1970; Lappin, Segal, Weatherburn, Henderson & Sykes, 1979; Farver, Blatt & Pecht, 1982; Gray, 1986; Sykes, 1985, 1988). From *e.g.* Cr^{III}-labelled azurin molecules, two seperate electron-transfer sites on azurin have been suggested, one for cytochrome c_{551} and another for nitrite reductase (Farver, Blatt & Pecht, 1982). The first site was identified as the surface close to His35. The second was a hydrophobic patch located around the copper ligand His117, also involved in the self-exhange reaction of azurin (Groeneveld & Canters, 1985, 1988). In later investigations the role of the His35 patch has been challenged and it has been concluded further that the His35 patch and His35, in particular, is not directly involved in the electron transfer, Van de Kamp, Floris, Hali & Canters (1990) have tentatively suggested that the hydrophobic patch around His117 in azurin is also involved in the electron-transfer reaction with cytochrome c_{551}.

Recently, the crystal structure of the ternary electron-transfer complex between a quinoprotein (methylamine dehydrogenase, MADH), a blue protein, amicyanin and a *c*-type cytochrome c_{551i} has been solved (Chen, Mathews, Davidson, Tegoni, Rivetti & Rossi, 1993). This structure reveals that the hydrophobic patch around the copper ligand His95 of amicyanin interacts with the active site of MADH. Based on these recent results, the surface of the azurin molecule, the pronounced hydrophobic patch at the northern end near the copper site, has also been considered as the main electron-transfer mediating surface (Nar, Messerschmidt, Huber, Kamp & Canters, 1991*a*; Baker, 1988). The His117 is bound to copper through $N^{\delta 1}$, with its imidazole ring on the surface. This imidazole ring is surrounded by the residues of Met13, Met44, Phe114, Pro115 and the methylene group of Gly116, which are all invariant in other azurins (Rydén & Lundgren, 1976). Phe114 is proximal to the ligand residue His117.

Hydrophobic, electrostatic and van der Waals forces are all involved in the various types of interactions made by the polypeptide chain of a protein. Thus, when structural data are available from X-ray crystallographic investigations the geometrical arrangement of molecular packing can be studied and, more specifically, the role of hydrophobicity can be assessed (Lee & Richards, 1971; Svensson *et al.*, 1991). From analysis of the structure of interfaces that occur between protein monomers it has been concluded the hydrophobicity is the major force in stabilizing protein–protein association, while van der Waals forces and hydrogen bonds play a selective role since they prevent incorrect associations by large unfavourable entropies (Chothia & Janin, 1975; Janin & Chothia, 1976, 1978). The packing of monomers to form dimers in the azurin system by joining the hydrophobic patches is an important object to study since it provides an insight into the plausible mechanism for the self-exchange electron transfer (Nar, Messerschmidt, Huber, van de Kamp & Canters, 1991*a*). We have, therefore, characterized the Phe114Ala mutant further and in this manuscript we report its crystal structure at 2.6 Å resolution from the *P. aeruginosa* bacteria. In addition, the packing of the monomers in relation to the hydrophobic patch is described and changes in the spectroscopic properties and reduction potential are interpreted as a consequence of the modified copper-site geometry.

Materials and methods

Site-directed mutagenesis and preparation of azurins

The mutant was constructed with the use of the oligonucleotide-directed *in vitro* mutagenesis system. *Escherichia coli* K12 TG1 (Carter, 1986) was used both for cloning and protein production. The plasmids pUC18/19 and M13mp18/19 were purchased from Boehringer-Mannheim. The plasmid pUG4 has been described by Karlsson, Aasa, Malmström & Lundberg (1989). The DNA technique, the production and the purification of the recombinant *P. aeruginosa* azurin and its mutants have also been described previously (Pascher, Bergström, Malmström, Vänngård & Lundberg, 1989).

Optical and EPR spectra and reduction potential

Optical spectra were recorded with a Shimadzu 3000 spectrophotometer. EPR spectra were obtained on a Bruker ER 20D-SRC spectrometer equipped with an Oxford Instrument using an EPR-9 helium cryostat. The optical spectra were recorded at a temperature of 293 K. Integrations were performed as described by Aasa & Vänngård (1975). All measurements were made in 100 m*M* KCl, 10 m*M* Hepes [4-(2-hydroxyethyl)-1-piperazineethane-sulfonic acid], pH 7.0. The EPR parameters were taken from an *S*-band spectra recorded at 77 K. The reduction potentials measured with the optically transparent thin-layer electrolysis technique were determined by Pascher, Karlsson, Nordling, Malmström & Vänngård (1993) at 298 K and using Tris(1,10-phenanthroline)cobalt(III) perchlorate as the redox mediator. Both the Phe114Ala azurin mutant and the mediator had concentration of 1 m*M*.

Crystallization and data collection

The blue well formed prismatic crystals of Phe114Ala crystrallized by utilizing the vapour-diffusion hanging-drop technique from a solution containing 25% PEG 4000, 0.2 *M* calcium chloride and 0.22 *M* acetate buffer at pH ≃ 6.0. The protein concentration was 7.5 to 10 mg ml^{-1}. The largest crystals were found in the dishes kept at 297–298 K, where each droplet contained 1–2 prismatically formed crystals of roughly 1.0 × 1.0 × 0.2 mm.

Two data sets for the Phe114Ala azurin mutant crystals were collected on two different diffractometers. One diffraction data set was collected at room temperature using a modified Syntex $P2_1$ automated four-circle diffractometer. A detailed description of the data collection and the data reduction for this data set had been presented previously (Tsai, Langer, Sjölin & Pascher, 1992).

The further X-ray data set was collected on a Xentronix area-detector system using Cu $K\alpha$ radiation from a Rigaku RU200 BH rotating anode operated at 40 kV and 80 mA with a 0.3 × 0.3 mm focal spot. A graphite monochromator together with a 0.5 mm collimator were also used. During the data collection the area-detector chamber was mounted 10.5 cm from the crystal and the data set was collected at room temperature. The individual frames were contiguous in that the beginning of each small oscillation range (0.1°) coincided with the end of the previous range. The determination of the unit-cell parameters, crystal orientation and the integration of reflection intensities were performed with the *XENGEN* program system (Howard, Gilliland, Finzel, Poulos, Ohlendorf & Salemme, 1987). The mutant Phe114Ala crystals belong to the monoclinic system and the space group has been determined as $P2_1$. The cell constants are $a = 51.0$, $b = 83.6$, $c = 66.4$ Å and $\beta = 110.5°$. 62110 reflections to a nominal resolution of 2.6 Å were collected with the area-detector system from one crystal, 14831 being unique. The data set represents 91% of the expected number of reflections at this resolution. For the entire data set 9573 reflections had $I > 3\sigma_I$, 10422 reflections had $I > 2\sigma_I$ and 11654 reflections had $I > \sigma_I$. The merging R_m factor was 7.1% for all the data to 2.6 Å resolution. The unique reflections were also analyzed using the program *LOAD* from the *PROTEIN* system (Steigemann, 1974), and some of the data-collection statistics are presented in Table 1. There are four molecules in the asymmetric unit and the calculated V_m value according to Matthews (1968) is 2.36 $Å^3$ Da^{-1}.

Structure solution and refinement

The structure of the azurin mutant Phe114Ala was solved by molecular replacement using the wild-type structure (Nar, Messerschmidt, Huber, van de Kamp & Canters, 1991*a*) as a search model. A self-rotation function computed within *PROTEIN* yielded a signal for local twofold symmetry axes at polar angles (90, 90, 180°) *e.g.* perpendicular to the *ab* plane and 20° off the crystallographic *c* axis, and at polar angles (90, 0, 180°), *e.g.* parallel to the crystallographic *a* axis. A check of the Patterson function revealed a pseudo-origin peak at $(u, v, w) = (0, 30/80, 33/66)$. This implied an arrangement of two dimers of almost identical orientation within the crystal asymmetric unit. A *PROTEIN* rotation function gave two clear peaks (2σ above the next highest peaks) at Euler angles (169, 43, 262°) and (9, 136, 80°). These orientations are related by the local twofold along the *a* axis. The translation component was determined using a translation function (Crowther & Blow, 1967) written by Lattman (1972) and modified by R. Huber & J. Deisenhofter (unpublished work). The function yielded a consistent set of self and cross vectors and positioned the two orientationally independent molecules at $(x, y, z) = (29/50, 66.1/80, 64/66)$ and (5.5/50, 0/80, 2.5/66). The azurin tetramer was then created by applying the Patterson pseudo-origin vector to the above positions and refined within *X-PLOR* (Brünger, 1991). An initial rigid-body refinement using data between 6 and 3 Å reduced the *R* factor from 55 to 39%. Subsequent positional and temperature-factor refinement resulted in an *R* factor of 25.4% for all data between

Table 1. *Data-collection parameters and statistics, the final model and refinement results for the Phe114Ala mutant*

	Data from Rigaku
Unit-cell constants (Å, °)	
a	51.0
b	83.6
c	66.4
β	110.5
Space group	$P2_1$
No. of molecules in asymmetric unit	4
Crystal mosaicity (°)	0.27
Total No. of measurements	62110
Total No. of unique reflections	14831
Data completeness (%)	91
Reflection averaging, R_m* (%)	7.1
No. of atoms used in refinement	4313
Protein atoms	3872
Solvent	441
Resolution range used in the refinement (Å)	8.0–2.60
No. of reflections in the resolution range	9832
No. of parameters	17253
Root-mean-square deviation	
Bonds (Å)	0.020
Angles (°)	2.0
R value†	18.5

* $R_m = \sum_H \sum_{i=1}^{N} |\langle I(H)\rangle - I(H)_i| / \sum_H \sum_{i=1}^{N} I(H)_i$. Where $I(H)_i$ is the *i*th measurement of reflection *H*, $\langle I(H)\rangle$ is its mean value and the summation extends over all the reflections measured more than once in the set.

† $R = \sum |F_o - F_c| / \sum |F_o|$.

8 and 2.6 Å. At that stage a $2F_o - F_c$ Fourier electron-density map was computed and the model was adjusted to the density where necessary. Special attention was paid to the mutation site which was omitted for phase calculations initially.

After two rounds of model building using *FRODO* (Jones, 1978) and refinement ($R = 24.5\%$), water molecules were added in places with high difference density and reasonable hydrogen-bond contacts and subsequently 240 water molecules were initially added to the coordinate list. The current model was further refined utilizing the *PROLSQ* program by (Hendrickson & Konnert, 1980) and the R factor decreased to 21.1% after 40 cycles of refinement and four modelling sessions on the computer graphics display. In addition, so-called maximum entropy electron-density maps were calculated and used as a complement to the regular $2F_o - F_c$ Fourier maps in each modelling cycle according to Sjölin, Svensson, Prince & Sundell (1990); Prince (1989); Sjölin & Svensson (1993). Using this procedure another 201 putative solvent molecules were chosen and, after 30 cycles of *PROLSQ* refinement and three supporting modelling sessions on the graphics display, the R factor was decreased to 18.7%.

At this stage the His117 side chains were removed in the four independent molecules forming a new coordinate set and an omit map was subsequently calculated and inspected. However, at the current resolution the orientation of these imidazole side chains could not be conclusively determined from the omit maps. Instead, the His117 side chains were again placed back in the copper site but now with the imidazole rings perpendicular to the copper-bond direction and the new coordinate set was consequently refined using *X-PLOR*. Simultaneously, the original coordinate set with the His117 imidazole rings positioned so that $N^{\delta 1}$ forms a bond with the copper ion was refined using the same parameter set-up in *X-PLOR*. After 25 cycles of temperature-factor refinement followed by 40 cycles of Powell minimization the R value for the latter coordinate set was 18.5% with a root-mean-square deviation for the atom positions of 0.020 Å.

Results

The final model of the Phe114Ala azurin mutant consists of 3868 protein atoms (four molecules) and 441 water molecules. The average isotropic temperature factor for the protein atoms is 26.1 Å^2, and the average temperature factor for the solvent atoms is 28.2 Å^2. Most of the structure is well defined, especially the β-strands, the loops around the copper site and all internal side chains. They have relatively low B factors of 5–20 Å^2. The N-terminal chains and residues 2–5 have higher B factors of 40–50 Å^2. The

Table 2. *The r.m.s. deviations calculated from a superposition of each of the four monomers A–D in the Phe114Ala azurin mutant*

The four r.m.s. values per block (Å) indicate values for C^α atoms, main-chain atoms, side-chain atoms and all atoms.

	A–B	*A–C*	*A–D*	*B–C*	*B–D*	*C–D*
C^α atoms	0.4719	0.5775	0.5649	0.5724	0.5013	0.4869
Main-chain atoms	0.5393	0.6076	0.6389	0.6369	0.5653	0.5554
Side-chain atoms	0.9056	0.9256	1.0122	1.0625	0.9842	0.9814
All atoms	0.7347	0.7736	0.8356	0.8637	0.7906	0.7852

$2F_o - F_c$ maps countoured at 1σ level show continuous density for all main-chain atoms.

A Ramachandran plot of the azurin model has been presented previously (Nar, Messerschmidt, Huber, van de Kamp & Canters, 1991*a*; Sjölin *et al.*, 1993), and it showed that nearly all residues lie in the allowable geometric regions. A plot of the temperature factor (B) *versus* the residues was made to check for regions of high mobility as well as to indicate the quality of the structure after the refinement (Fig. 1). A comparison of the four monomers in the asymmetric unit suggests that the deviation from the main-chain atom positions is small in the structure. The mean deviations for the main-chain atom positions range between 0.54 and 0.64 Å, and between 0.91 and 1.06 Å for the side-chain positions. The r.m.s. differences between the four monomers are presented in Table 2.*

The crystal form of the *P. aeruginosa* azurin mutant Phe114Ala contains eight molecules in the unit cell. The four molecules in the asymmetric unit are packed as a dimer of dimers. The crystal packing is visualized with a C^α skeleton drawing in Fig. 2.

* Atomic coordinates and structure factors have been deposited with the Protein Data Bank, Brookhaven National Laboratory. Free copies may be obtained through The Managing Editor, International Union of Crystallography, 5 Abbey Square, Chester CH1 2HU, England (Reference: 1AZN, R1AZNSF). A list of deposited data is given at the end of this issue.

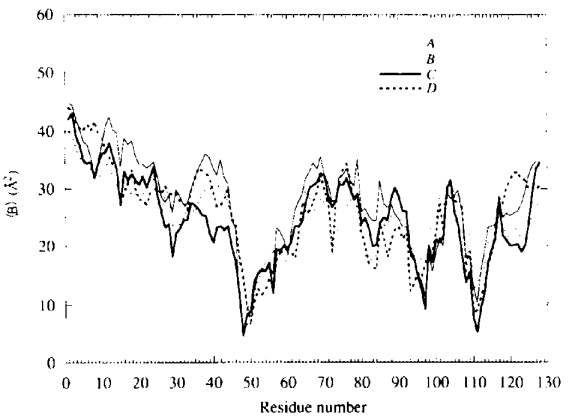

Fig. 1. The average temperature factor as a function of amino-acid residue number of the monomers *A*, *B*, *C* and *D*.

The dimer contact region is constructed so that the monomers are attached by their hydrophobic patches surrounding the amino-acid residue His117. The hydrophobic patch consisting of residues Met13, Leu39, Pro40, Val43, Met44, Ala114, Pro115, Gly116, Ala119 and Leu120 is viewed in Fig. 3. The closest contacts between the two hydrophobic patches in the dimer involve main-chain and side-chain contacts for the amino-acid residues 115 and 116. It is interesting to note that the packing of the dimer in this mutant is very similar to the dimer packing in the *Alcaligenes denitrificans* azurin structure (Baker, 1988). A view of the C^{α} atoms in the Ala114 azurin mutant superimposed on the *A. denitrificans* azurin dimer is illustrated in Fig. 4. In the latter structure as well as in the current Ala114-mutant structure one water molecule forms a bridge between His117 N^{ε} in monomer *C* and Gly116 O in monomer *D* (Fig. 5). This water bridge has been considered important for the electron self-reaction mechanism. However, the *P. aeruginos* azurin crystallized from ammonium sulfate also forms dimers in the crystalline phase but the monomers are packed differently in spite of the fact that they still are attached through their hydrophobic patches. In this dimer construct, two water molecules form a bridge in the *P. aeruginosa* azurin structure but now between the two His117 N^{ε} atoms from the two monomers (Nar, Messerschmidt, Huber, Kamp & Canters, 1991*a*). This is, consequently, another possible route for the electron self-exchange reaction as indicated previously by Nar, Messerschmidt, Huber, van de Kamp & Canters (1991*a*).

The two crystallographically independent dimers in the current structure are packed together so that residues 8, 12–14, 36 and 38 in monomer *A* are in contact with residues 6, 8, 14–17 in monomer *C*. Monomers *B* and *C* are in contact with each other *via* residues 14 and 8, respectively. There is no contact surface between monomers *A* and *D* or between monomers *B* and *D*. The intermolecular hydrogen bonds are listed in Table 3.

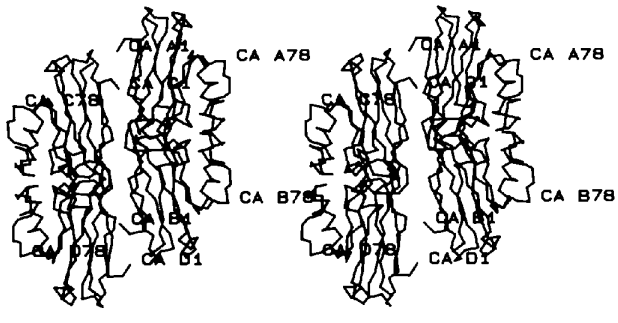

Fig. 2. A drawing of the C^{α} atoms in the four crystallographically independent azurin Phe114Ala molecules. The *AB* dimer is shown to the right, the *CD* dimer to the left.

Table 3. *Intermolecular hydrogen bonds*

*A*28 Gln $N^{\varepsilon 2}$···O Ala53 *B*^{i}	*B*28 Gln $N^{\varepsilon 2}$···O Ala53 *A*^{v}
*A*53 Ala O···$N^{\varepsilon 2}$ Gln28 *B*^{ii}	*B*53 Ala O···$N^{\varepsilon 2}$ Gln28 *A*^{vi}
*A*78 Ser O^{γ}···Asn16 *D*^{i}	*B*96 Thr O···$N^{\varepsilon 2}$ Gln107 *A*^{v}
*A*96 Thr N···$O^{\varepsilon 1}$ Gln107 *B*^{i}	*B*96 Thr N···$O^{\varepsilon 1}$ Gln107 *A*^{v}
*A*96 Thr $O^{\gamma 1}$···$O^{\varepsilon 1}$ Gln107 *B*^{i}	*B*107 Gln $O^{\varepsilon 1}$···N Thr96 *A*^{vi}
*A*107 Gln O^{ε}···N Thr96 *B*^{ii}	*B*107 Gln $N^{\varepsilon 2}$···O Thr96 *A*^{vi}
*A*107 Gln $N^{\varepsilon 2}$···O Thr96 *B*^{ii}	
	*D*16 Asn O···O^{γ} Ser78 *A*^{vi}
*C*28 Gln $N^{\varepsilon 2}$···O Ala53 *D*^{iii}	*D*53 Ala O···$N^{\varepsilon 2}$Gln28 *C*^{vii}
*C*28 Gln $N^{\varepsilon 2}$···$O^{\varepsilon 1}$ Gln57 *D*^{iii}	*D*57 Gln $O^{\varepsilon 1}$···$N^{\varepsilon 2}$ Gln28 *C*^{vii}
*C*96 Thr N···$O^{\varepsilon 1}$ Gln107 *D*^{iii}	*D*96 Thr O···$N^{\varepsilon 2}$ Gln107 *C*^{viii}
*C*107 Gln $O^{\varepsilon 1}$···$O^{\gamma 1}$ Thr96 *D*^{iv}	*D*96 Thr $O^{\gamma 1}$···$O^{\varepsilon 1}$ Gln107 *C*^{viii}
*C*107 Gln $N^{\varepsilon 2}$···O Thr96 *D*^{iv}	*D*107 Gln $OP^{\varepsilon 1}$···N Thr96 *C*^{vii}
*A*8 Gln $N^{\varepsilon 2}$···O Ala*C*19	*A*38 Asn $O^{\delta 2}$···$N^{\varepsilon 2}$ Gln*C*14
*A*12 Gln $N^{\varepsilon 2}$···$O^{\varepsilon 1}$ Gln*C*8	*A*115 Pro O···N Gly*B*116
*A*12 Gln $O^{\varepsilon 2}$···$N^{\delta 2}$ Asn*C*16	*B*14 Gln $N^{\varepsilon 2}$···$N^{\varepsilon 2}$ Gln*C*8
*A*14 Gln $N^{\varepsilon 2}$···$O^{\delta 2}$ Asp*C*6	*D*115 Pro O···N Gly*C*116
*A*38 Asn $N^{\delta 2}$···$O^{\varepsilon 2}$ Gln*C*14	

Symmetry operators: (i) $1-x$, $1/2+y$, $2-z$; (ii) $2-x$, $1/2+y$, $2-z$; (iii) $1-x$, $1/2+y$, $1-z$; (iv) $-x$, $1/2+y$, $1-z$; (v) $2-x$, $y-1/2$, $2-z$; (vi) $1-x$, $y-1/2$, $2-z$; (vii) $1-x$, $y-1/2$, $1-z$; (viii) $-x$, $y-1/2$, $1-z$.

The site-specific mutation was undertaken at position Phe114 and this residue is situated in the hydrophobic patch and close to the copper ligand, His117. In fact, in the wild-type protein, the Phe114 amino-acid residue exhibits a π-electron overlap with the imidazole ring of His117. Fig. 6 shows a superposition of the current structure and coordinates from the *P. aeruginosa* wild-type azurin structure.

The copper sites in different azurins have been described previously and discussed in detail by Baker (1988) and by Nar, Messerschmidt, Huber, Kamp & Canters (1991*b*). The copper site of this mutant appears to be somewhat different since the Cu—$N^{\delta 1}$ (His117) bond is extended by *ca* 0.4 Å while the other Cu bonds are rather similar to those obtained in the wild-type structure as seen in Table 4. The overall change for the His117 imidazole ring is not surprising since this side chain obtains more rotational and translational freedom when there is no longer a phenylalanine ring behind it. An inspection of the $2F_o - F_c$ maps in this region reveals that there is no continuous density between either the $N^{\delta 1}$ and the copper ion or between the C^{β} and C^{γ} of this residue indicating the inherently higher flexibility (Fig. 7). In fact, the positioning of the imidazole rings based on the $2F_o - F_c$ maps is not unambiguous since the density around these side chains is approximately spherical in shape. The calculated omit maps did not indicate any preferred orientation of these side chains either. Instead, the positions currently chosen are based on a clear tendency obtained from the *X-PLOR* refinement where the side chains were initially positioned perpendicular to the bond direction. After convergence all four crystallographically independent His117 side chains had rotated to form a Cu—$N^{\delta 1}$ bond.

Table 4. *Copper-site geometry in the four monomers A–D from the azurin mutant Phe*114*Ala*

The average distance is also indicated as well as the tabulated wild-type values.

(*a*) Cu ligand bond length (Å)

	A	*B*	*C*	*D*	Average	Azurin (pH 5.5)
Cu—O (45)	3.06	2.78	3.07	3.03	2.99	2.97
Cu—$N^{\delta 1}$ (46)	2.16	2.05	2.21	2.09	2.19	2.11
Cu—S^{γ} (112)	2.24	2.24	2.22	2.22	2.23	2.25
Cu—$N^{\delta 1}$ (117)	2.64	2.46	2.36	2.38	2.46	2.03
Cu—S^{δ} (121)	2.86	3.11	3.01	3.12	3.04	3.15

(*b*) Bond angle around copper (°)

	Phe114Ala	Azurin (pH 5.5)
(45) O—Cu—$N^{\delta 1}$ (46)	76	79
(45) O—Cu—S^{γ} (112)	80	107
(45) O—Cu—N^{δ}1 (117)	78	92
(45) O—Cu—S^{δ} (121)	154	147
(46) $N^{\delta 1}$—Cu—S^{γ} (112)	140	128
(46) $N^{\delta 1}$—Cu—$N^{\delta 1}$ (117)	105	107
(46) $N^{\delta 1}$—Cu—S^{δ} (121)	80	70
(112) S^{γ}6—Cu—$N^{\delta 1}$ (117)	98	123
(112) S^{γ}—Cu—S^{δ} (121)	124	100
(117) $N^{\delta 1}$—Cu—S^{δ} (121)	99	86

The spectroscopic characteristics of the Ala114 mutant indicate that the copper site is perturbed with a shift in the charge-transfer band to a shorter wavelength by 7 nm and a small decrease in the copper hyperfine splitting is also detected. In addition, the reduction potential is increased by 20–50 mV depending on the different media used in the investigation (Pascher, Karlsson, Nordling, Malmström & Vänngård, 1993). The spectroscopic and redox data are presented in more detail in Table 5. The change in the reduction potential is presumably an indication of the alternation previously described for the copper site. Since Cu^{I} is spectroscopically silent in the EPR spectra, the copper ion must possess the oxidation state +2 in our crystal.

Discussion

In cupredoxins the copper ion functions as the locus for the electron. It is reduced from Cu^{II} to Cu^{I} on uptake of one electron and oxidized from Cu^{I} to Cu^{II} on release of the electron. In all known structures of cupredoxins the Cu atom is bound at the same end of a β-barrel with one of its ligands, the histidine ring, exposed at the surface of the protein. A number of pathways for the electron to enter or leave the copper have previously been suggested. However, the hydrophobic patch and subsequently the surface-ligand histidine are natural candidates for the electron transfer in all cupredoxins. The partners and a detailed description of the electron-transfer sites are not known for most of these proteins. For plastocyanin, on the other hand, there are strong indications that the electron delivered from cyto-

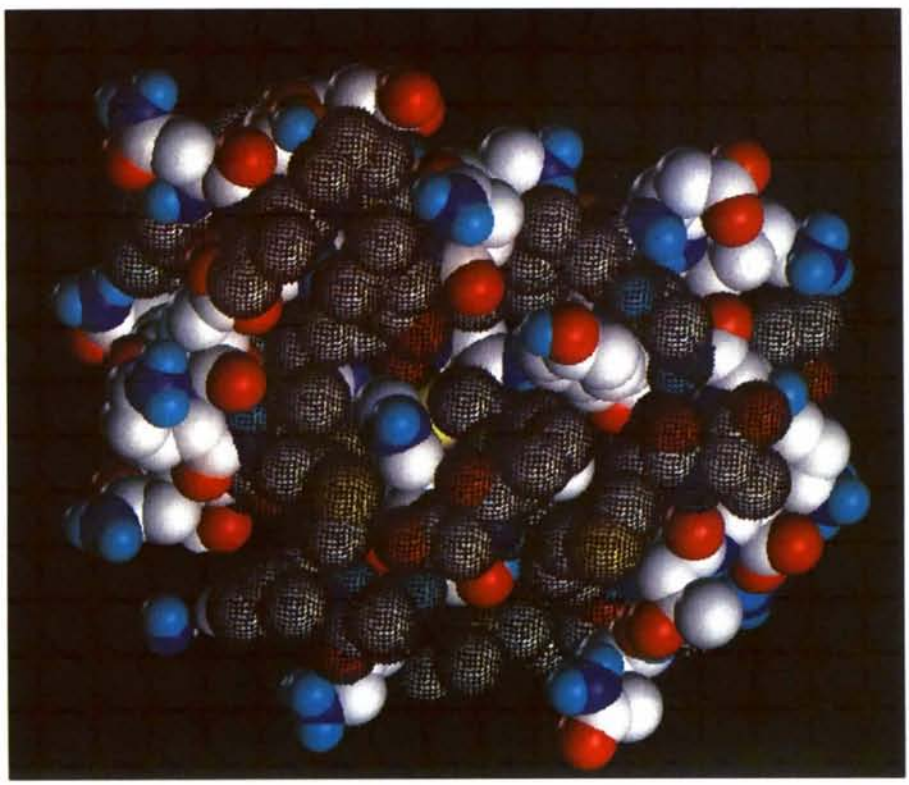

Fig. 3. A view of the northern end of the Phe114Ala azurin mutant structure where amino-acid residues which belong to the hydrophobic patch are indicated by the bluish grid pattern. The side chains of the polar amino-acid residues Tyr71 and His117 are clearly seen within the hydrophobic patch as well as the carbonyl O atom of Gly116.

chrome *f* enters through the Tyr83 residue but when the electron is released it exits through the surface ligand His84. For azurin the overall picture is more complicated. There is a cytochrome (cytochrome c_{551}) which in the bacteria, can replace azurin and even exchange electrons in both directions with azurin. Both proteins are supposed to accept electrons from the bc_1 complex and donate them to nitrite reductase. Most evidence at present suggests that azurin exchanges electrons only through the surface ligand His117 or the carbonyl O atom of Gly116. Interestingly, the mutation Phe114Ala has no significant effect on the self-exchange electron-transfer rate (Farver *et al.*, 1993) despite the fact that this mutation leaves more freedom for His117 and in the crystal structure it adopts a position relative to the Cu atom which is significantly different.

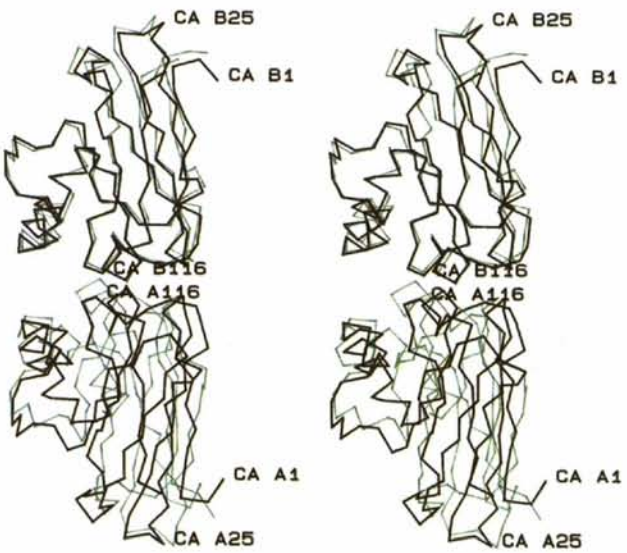

Fig. 4. A super position of C^{α} atoms from the Phe114Ala *AB* dimer (black lines) on the *Alcaligenes denitrificans* azurin dimer (green lines).

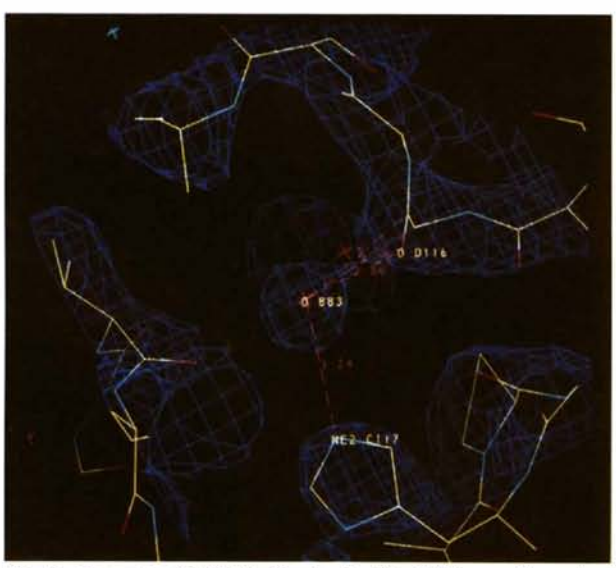

Fig. 5. The water (O 883) bridge in the Phe114Ala azurin mutant dimer between His117 N^{ϵ} in monomer *C* and the carbonyl O atom of Gly116 in monomer *D*.

Table 5. *Optical and EPR properties of wild-type azurin and azurin mutants Phe115Ala and Phe114Val and reduction potentials*

(*a*) Optical and EPR properties

Protein	EPR Parameters g/g_z	A	g	λ_{max} (nm)	ε ($M^{-1}cm^{-1}$)
Wild-type	2.259	50	2.059	627.0	5500
Phe114Ala	2.246	53	2.051	617.5	4300
Phe114Val	2.237	52	2.058	617.0	6000

(*b*) Reduction potentials

Protein	E°(mV) 0.1 *M* KCl/10 m*M* Hepes* pH 7.0
Wild type	310
Phe114Ala	358
Phe114Val	324

* Hepes, 4-(2-hydroxyethyl)-1-piperazineethane-sulfonic acid.

The spectral characteristics of the Ala114 azurin mutant is, on the other hand, somewhat changed as compared to the wild-type azurin characteristics (Pascher, Bergström, Malmström, Vänngård & Lundberg, 1989). The mutant displays a decrease in the hyperfine splitting by 4×10^{-4} cm^{-1} and an increase of about 50 mV in the reduction potential. The Ala114 mutant also exhibits a change in the charge-transfer band to a shorter wavelength by approximately 7 nm. However, the second-order rate constant of the reaction with cytochrome c_{551} is similar to the wild-type rate constant. Another Phe114 mutant, Val114 as a comparison, shows the same characteristic as the Ala114 mutant except that the reduction potential only rises by *ca* 15 mV (Pascher, Karlsson, Nordling, Malmström & Vänngård, 1993). A possible cause could be that the Phe114 restricts the mobility of the imidazole side chain of the ligand His117, with which it is in van der Waals contact, whereas the mobility is increased in the mutants. The smaller effect with mutant Val114 compared to Ala114 would then arise from a partial steric hindrance provided by the longer side chain.

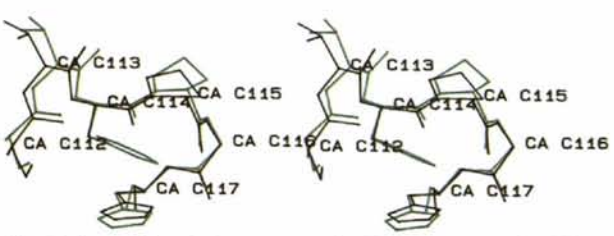

Fig. 6. An overlay of the structure Phe114Ala mutant (black lines) and the wild-type (green lines) structure at the mutation site.

These small differences in the spectral characteristics of the Ala114 azurin mutant can presumably be attributed to the change in the His117 potential only. The increased reduction potential of this mutant is probably due to the fact that the driving force of the long-range electron transfer (LRET) is changed upon the substitution in position 114. This assumption has previously been adopted in theoretical calculations by Farver *et al.* (1993). The mutation Phe114Ala has relatively little effect on the self-electron transfer rate, indicating that the position 114 attributes a general addition to the hydrophobic patch only and the position is not really involved in the electron transfer itself as compared to the substantially decreased reduction potential for the mutation Met44Lys reported before by van de Kamp, Silvestrini, Brunori, Beeumen, Hali & Canters (1990).

When a small molecule or a protein molecule binds to, or associates with, another protein molecule they lose, to some extent, translation and rotational freedom. For the binding of a small molecule, this loss has previously been estimated to be *ca* 71–92 kJ mol^{-1} (17–22 kcal mol^{-1}) in the standard state. On the other hand, the reduction of surface area which occurs when the complex forms is a source of favourable free energy. Chothia (1974) showed that there is a linear relationship between accessible surface areas of amino-acid residues and the free-energy changes associated with the transfer of the amino acids from water to organic solvent. The slope of this line corresponds to a free-energy change of about 104 J $Å^{-2}$ (25 cal $Å^{-2}$) for non-polar residues. In protein–protein complexes, which bury 1500 $Å^2$ or more of the hydrophobic surface, this has been shown to account for the stability of association (Chothia & Janin, 1975; Janin & Chothia, 1976). However, the hydrophobicity probably only accounts for the association while the specificity in binding is mediated by van der Waals forces and complementary hydrogen bonds (*cf.* Fig. 4).

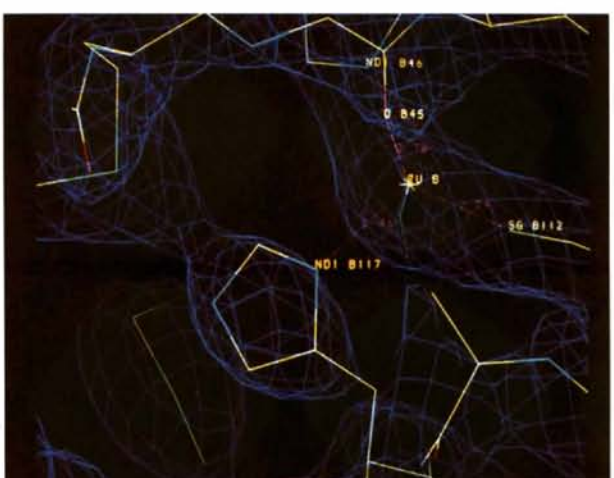

Fig. 7. $2F_o - F_c$ Fourier electron-density map for the copper site in the Phe114Ala mutant showing no continuous density between the Cu atom and $N^{\delta 1}$ His117 and showing weak density only between C^{β} and C^{γ}.

The hydrophobic patch in the related protein plastocyanin, as a comparison, is made up of eight small non-polar amino-acid residues that are all conserved in the eukaryotic system and the hydrophobic patch is remarkably flat in shape. Calculations of the solvent-accessible surface area (Conolly, 1983) of these conserved residues in the hydrophobic patch revealed that they make up *ca* 550 $Å^2$ of the molecular surface area. Plastocyanin and its mutants are notoriously difficult to crystallize and dimer formation mediated by the hydrophobic patch is rare, probably because of the small size of this surface.

In the case of the formation of azurin dimers the hydrophobic patch is seemingly large enough to associate two molecules in a 'north pole'-to-'north pole' configuration. The specificity for the association is, however, not very large as compared to *e.g.* binding of coenzymes or substrate in other protein systems, since we can observe at least two different geometries for the monomers forming the dimer in different azurin and azurin-mutant structures. The consequence of this observation is that the self-exchange electron transfer probably follows more than one specific mechanism. Maybe this lesser specificity makes a self-exchange electron transfer less probable compared with normal electron-exchange transfer mediated by the regular redox partners of azurin which, in this situation, should associate with the azurin molecule with a higher degree of specificity.

We would like to thank the Swedish Natural Science Research Council and the Bio-Väst Foundation for Biotechnology for financial support of this project. Professors B. G. Malmström and Tore Vänngård and Dr Göran Karlsson are acknowledged for many stimulating discussions concerning blue-copper proteins in general and this work in particular.

References

Aasa, R. & Vänngård, T. (1975). *J. Magn. Reson.* **19**, 308–315.
Adman, E. T. (1991). *Adv. Protein Chem.* **43** 145–197.
Adman, E. T. & Jensen, L. (1981). *Isr. J. Chem.* **21**, 8–12.
Antonini, E., Finazzi-Agro, A., Avigliano, L., Guerrieri, P., Rotilio, G. & Mondovi, B. (1970). *J. Biol. Chem.* **245**, 4847–4856.
Baker, E. N. (1988). *J. Mol. Biol.* **203**, 1071–1095.
Brünger, A. T. (1991). *Annu. Rev. Phys. Chem.* **42**, 197–223.

CARTER, P. (1986). *Biochem. J.* **237**, 1–7.
CHEN, L. Y., MATHEWS, F. S., DAVIDSON, V. L., TEGONI, M., RIVETTI, C. & ROSSI, G. L. (1993). *Protein Sci.* **2**, 147–154.
CHOTHIA, C. (1974). *Nature (London)*, **248**, 338–339.
CHOTHIA, C. & JANIN, J. (1975). *Nature (London)*, **256**, 705–708.
CONOLLY, M. L. (1983). *J. Appl. Cryst.* **16**, 548–558.
CROWTHER, R. A. & BLOW, D. M. (1967). *Acta Cryst.* **23**, 544–548.
FARVER, O., BLATT, Y. & PECHT, I. (1982). *Biochemistry*, **21**, 3556–3561.
FARVER, O., SKOV, L. K., PASCHER, T., KARLSSON, B. G., NORDLING, M., LUNDBERG, L., VÄNNGÅRD, T. & PECHT, I. (1993). *J. Am. Chem. Soc.* **32**, 7317–7322.
GRAY, H. B. (1986). *Chem. Soc. Rev.* **15**, 17–30.
GRAY, H. B. & MALMSTRÖM, B. G. (1983). *Comments Inorg. Chem.* **2**, 203–209.
GROENEVELD, C. M. & CANTERS, G. W. (1985). *Eur. J. Biochem.* **153**, 559–564.
GROENEVELD, C. M. & CANTERS, G. W. (1988). *J. Biol. Chem.* **263**, 167–173.
GUSS, J. M. & FREEMAN, H. C. (1983). *J. Mol. Biol.* **129**, 521–563.
HENDRICKSON, W. A. & KONNERT, J. H. (1980). *Acta Cryst.* A**36**, 344–350.
HOWARD, A. J., GILLILAND, G. L., FINZEL, B. C., POULOS, T. L., OHLENDORF, D. H. & SALEMME, F. R. (1987). *J. Appl. Cryst.* **20**, 383–387.
JANIN, J. & CHOTHIA, C. (1976). *J. Mol. Biol.* **100**, 197–211.
JANIN, J. & CHOTHIA, C. (1978). *J. Am. Chem. Soc.* **17**, 2943–2948.
JONES, T. A. (1978). *J. Appl. Cryst.* **11**, 268–272.
VAN DE KAMP, M., FLORIS R., HALI, F. C. & CANTERS, G. W. (1990). *J. Am. Chem. Soc.* **112**, 907–908.
VAN DE KAMP, M., SILVESTRINI, M. C., BRUNORI, M., BEEUMEN, J. V., HALI, F. B. & CANTERS, G. W. (1990). *Eur. J. Biochem.* **194**, 109–118.
KARLSSON, B. G., AASA, R., MALMSTRÖM, B. G. & LUNDBERG, L. G. (1989). *FEBS Lett.* **253**, 99–102.
KARLSSON, B. G., TSAI, L. C., NAR, H., LANGER, V. & SJÖLIN, L. (1994). *J. Biol. Chem.* Submitted.
LAPPIN, A. G., SEGAL, M. G., WEATHERBURN, D. C., HENDERSON, R. A. & SYKES, A. G. (1979). *J. Am. Chem. Soc.* **101**, 2302–2306.
LATTMAN, E. E. & LOVE, W. E. (1972). *Acta Cryst.* B**26**, 1854–1857.
LEE, B. K. & RICHARDS, F. M. (1971). *J. Mol. Biol.* **55**, 379–400.
MATTHEWS, B. W. (1968). *J. Mol. Biol.* **33**, 491–497.
MESSERSCHMIDT, A. & HUBER, R. (1990). *Eur. J. Biochem.* **187**, 341–345.
NAR, H., MESSERSCHMIDT, A., HUBER, R., VAN DE KAMP, M. & CANTERS, G. W. (1991*a*) *J. Mol. Biol.* **218**, 427–447.
NAR, H., MESSERSCHMIDT, A., HUBER, R., VAN DE KAMP, M. & CANTERS, G. W. (1991*b*). *J. Mol. Biol.* **221**, 765–776.
NORINDER, U., SJÖLIN, L., PASCHER, T. & KARLSSON, B. G. (1994). *J. Biol. Chem.* Submitted.
NORRIS, G. E., ANDERSON, B. E. & BAKER, E. N. (1986). *J. Am. Chem. Soc.* **108**, 2784–2785.
PASCHER, T., BERGSTRÖM, J., MALMSTRÖM, B. G., VÄNNGÅRD, T. & LUNDBERG, L. G. (1989). *FEBS Lett.* **258**, 266–268.
PASCHER, T., KARLSSON, B. G., NORDLING, M., MALMSTRÖM, B. G. & VÄNNGÅRD, T. (1993). *Eur. J. Biochem.* **212**, 289–296.
PRINCE, E. (1989). *Acta Cryst.* A**45**, 200–203.
RYDÉN, L. (1988). *Prog. Clin. Biol. Res.* **274**, 349–366.
RYDÉN, L. & LUNDGREN, J. O. (1976). *Nature (London)*, **261**, 344–346.
SJÖLIN, L. & SVENSSON, L. A. (1993). *Acta Cryst.* D**49**, 66–74.
SJÖLIN, L., SVENSSON, L. A., PRINCE, E. & SUNDELL, S. (1990). *Acta Cryst.* B**46**, 209–215.
SJÖLIN, L., TSAI, L. C., LANGER, V., PASCHER, T., KARLSON, B. G., NORDLING, M. & NAR, H. (1993). *Acta Cryst.* D**49**, 449–457.
STEIGEMANN, W. (1974). PhD thesis, Technische Univ., München, Germany.
SVENSSON, L. A., DILL, J., SJÖLIN, L., WLODAWER, A., TONER, M., BACON, D., MOULT, J., VERRAPANDIAN B. & GILLILAND, G. L. (1991). *J. Cryst. Growth*, **110**, 119–130.
SYKES, A. G. (1985). *Chem. Soc. Rev.* **14**, 283–315.
SYKES, A. G. (1988). *Chem. Br.* pp. 551–554.
TSAI, L. C., LANGER, V., SJÖLIN, L. & PASCHER, T. (1992). *Acta Cryst.* B**48**, 107–109.